Images of Jupiter's Sulfur Ring

Abstract. *Images of the ring of singly ionized sulfur encircling Jupiter obtained on two successive nights in April 1979 show that the ring characteristics may change dramatically in ~ 24 hours. On the first night the ring was narrow and confined to the magnetic equator inside Io's orbit. On the second it was confined symmetrically about the centrifugal symmetry surface and showed considerable radial structure, including a "fan" extending to Io's orbit. Many of the differences in the ring on the two nights can be explained in terms of differences in sulfur plasma temperature.*

Jupiter's innermost Galilean satellite, Io, appears to be the source of a host of atomic and perhaps molecular nebulae that are distributed around the inner Jovian magnetosphere. Ground-based observations of circum-Jovian space have revealed optical emissions of neutral sodium (*1*) and potassium (*2*), and singly ionized sulfur (*3*) and oxygen (*4*). Optical instruments on spacecraft have detected emissions of doubly and triply ionized sulfur (*5*), doubly ionized oxygen (*5*), and (perhaps) neutral hydrogen (*6*). The Voyager 1 plasma experiment also provided evidence for S^+, S^{2+}, O^+, and O^{2+}, and for S_2^+ or SO_2^+ or both (*7*). Of the emissions that can be measured from the ground, those of sulfur and oxygen are particularly interesting from a magnetospheric standpoint because they arise from the de-excitation of metastable, collisionally excited states. The populations and de-excitation rates of these states depend on the characteristics of the ambient thermal plasma (*8*). Measurements of these forbidden emissions thus provide a valuable tool for studies of this plasma and the inner Jovian magnetosphere.

Early reports that the S^+ emission was confined to a disk with a void around Io (*3, 9*) were later shown to be erroneous. Pilcher and Morgan (*10, 11*) found the S^+ emission to be confined to a toroidal region around the Jovian magnetic equator. They also found the emission to vary in intensity with longitude, often appearing brightest in the "active" sector, the range of magnetic longitudes over which Io is capable of modulating the Jovian decametric emission (*12*). Toroidal distributions of S^+ emission were also found by Brown (*13*) and Trauger *et al.* (*14*); the latter also found evidence for magnetic equatorial confinement. The thickness of the sulfur ring has generally been quoted as 1 to 2 Jupiter radii (R_J) (*3, 9–11, 15*), although there has been some evidence that the thickness varies with apparent radial distance from Jupiter (*11*). Nash (*16*) combined much of the previously available ground-based data to conclude that the ring is "wedge-shaped . . . encircling Jupiter along the magnetic equator between radii 4.3 and 7.2 R_J, with inner thickness 0.4 and outer thickness 1.4 R_J. Both radii and thickness vary with time and longitude."

In this report I present photographic images of the circum-Jovian ring of S^+ obtained with the 2.2-m telescope at Mauna Kea Observatory. To my knowledge, these data are the first to illustrate the spatial extent and short-term temporal variability of the S^+ emission. The images were obtained by means of a simple optical system including a collimating lens, narrowband (~ 3 Å) interference filter, reimaging lens, and an RCA Carnegie two-stage magnetically focused image intensifier. The interference filter passband at normal incidence was centered a few angstroms to the red of the S^+ forbidden line at 6731 Å. The filter was then "tuned" to the actual wavelength of the Doppler-shifted emission by tilting. All of the images presented here were 15-minute exposures on Kodak IIa-0 plates.

Images obtained on 9 and 10 April 1979 (universal time) are shown in Figs. 1 and 2, respectively. The images are all nominally centered 5.6 R_J from Jupiter in the planet's rotational equator (*17*). On both nights, Io was on the opposite side of the planet from the side corresponding to the images. A ring of radius 5.3 R_J in the planet's magnetic equator was chosen for illustration in Fig. 1 because it provides a good overall match to the images obtained on the first night (*18*). The image in Fig. 1A is shown displaced ~ 5 arc seconds south of its nominal center. This displacement was necessary to obtain reasonable agreement with a ring in the magnetic equator; better agreement still can be obtained with a slightly smaller (~ 5.0 R_J) magnetic equatorial ring. The image in Fig. 1B is matched extremely well by a ring of radius 5.3 to 5.4 R_J in the magnetic equator if it is assumed that the image is centered 1 to 2 arc seconds south of its nominal position (as shown). The image in Fig. 1C is matched well by a magnetic equatorial ring of radius 5.3 to 5.5 R_J if this image is also assumed to lie ~ 5 arc seconds south of its nominal center. The requirement that these images all be moved slightly south of their nominal positions for best agreement probably reflects telescope pointing inaccuracies. An upper limit to the thickness of the ring on this night obtained from Fig. 1, A and C, is 0.3 R_J.

The ring had an entirely different appearance on the following night (Fig. 2). Figure 2A shows a much more diffuse ring of radius ~ 5.7 R_J, with a linear brightening at the ansa and an inclination to the rotational equator of only 7° ± 1°. This image was made 24 hours and 18 minutes after that in Fig. 1A, an interval just 29 minutes less than 2½ times the Jovian rotation period, and thus shows essentially the same magnetic longitudes as the earlier image. The image in Fig. 2B, made 1 hour and 42 minutes after that shown in Fig. 2A, shows that on this night the ring had a cross section in the shape of a wedge or a fan. The outer edge of the fan is 5.9 R_J from Jupiter (Io's orbital distance) and is inclined slightly to the Jovian rotational axis. Its apex is ~ 5 R_J from the planet and is centered in a concentration in the emission that extends from ~ 4.7 to ~ 5.2 R_J. The ring in this image is also inclined 7° ± 1° to the rotational equator. The linear brightening at the ring ansa shown in Fig. 2A is most likely an effect of the viewing geometry and the presence of the fan. An image obtained to the east of Jupiter on this night and reproduced elsewhere (*19*) also showed a 7° inclination and a range of magnetic longitudes relatively free of emission, as previously observed by Pilcher and Morgan (*10, 11*).

The key to the differences in the sulfur ring on the two nights lies in the difference in the ring inclination. Siscoe (*20*) has shown that ions formed from the neutrals originating on a Galilean satellite are confined by magnetic forces symmetrically about the magnetic equator at radial distances from Jupiter less than or equal to the orbital distance of the satellite. At larger distances, centrifugal forces dominate and the ions are confined instead to a "centrifugal symmetry surface," consistent with the analysis of Hill and Michel (*21*). The transition between magnetic and centrifugal confinement occurs at the satellite's orbital distance only if the ions retain their initial velocity perpendicular to the magnetic field lines. This velocity is given by the difference between the neutrals' Keplerian velocity prior to ionization and the corotation velocity of the magnetic field, a difference equal to 56 km/sec for neutrals originating on Io. As the ion velocity (**v**) decreases from this value because of collisions, the transition region moves closer to Jupiter; that is, **v** × **B** forces (where **B** is the magnetic field strength) become less important relative to rotational forces. Hill *et al.* (*22*) have shown

 0036-8075/80/0111-0181$00.50/0

that if the Jovian magnetic field in this region is dipolar, its 10.6° tilt will yield a centrifugal symmetry surface inclined 7° to the rotational equator, a value in exact agreement with the measured inclination of the sulfur ring on the second of the two nights. A major part of the difference between the rings on the two nights thus appears to be due to a difference in ion kinetic temperature: on the first night the ring was "hot" and confined to the magnetic equator, on the second it was "cold" and confined to the centrifugal symmetry surface.

For a cold ring, the thickness of the ion distribution about the symmetry surface is dependent on the mean ion velocity parallel to the field lines (*21*). The fan in Fig. 2B can thus be interpreted as due to a radial temperature gradient in the ring. The total north-south extent of the fan at its outermost edge ($5.9 R_J$ from Jupiter) is $\sim 1.1 R_J$. This corresponds to an ion temperature parallel to the field lines of ~ 24 eV (*21*). The fan thickness decreases linearly, implying a linear decrease in ion velocity, until it reaches a minimum at $\sim 5.1\ R_J$ from Jupiter of $\lesssim 0.3 R_J$, corresponding to an ion parallel temperature of $\lesssim 2$ eV. The outer edge of the fan most likely marks the plasma temperature discontinuity observed near the Io torus in the Voyager 1 plasma experiment. Outside that boundary, ion temperatures were found to be in excess of 25 eV and the dominant form of sulfur was S^{2+} (*5, 7*). Inside that boundary, ion temperatures were as low as ~ 1 eV and S^+ was abundant (*7*).

The Voyager ultraviolet spectrometer results have shown that the plasma torus may radiate rapidly enough to cool hot, newly ionized material from Io on the time scale implied by these observations (*5, 23*). Alternatively, both hot and cold

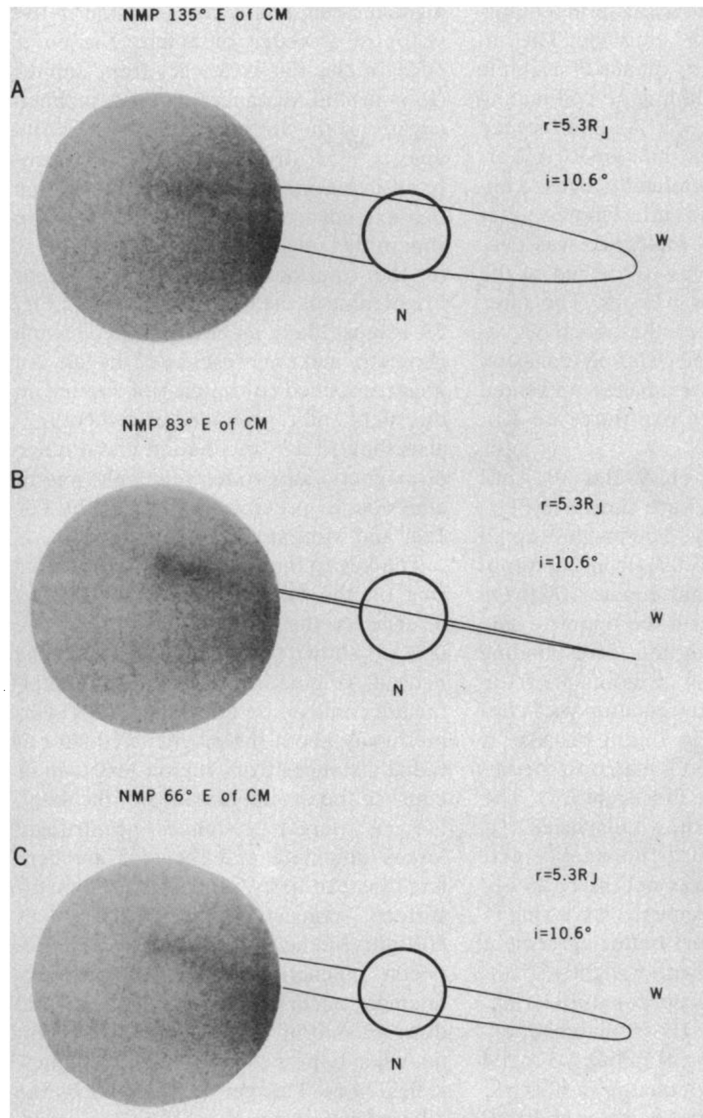

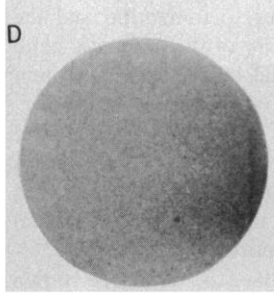

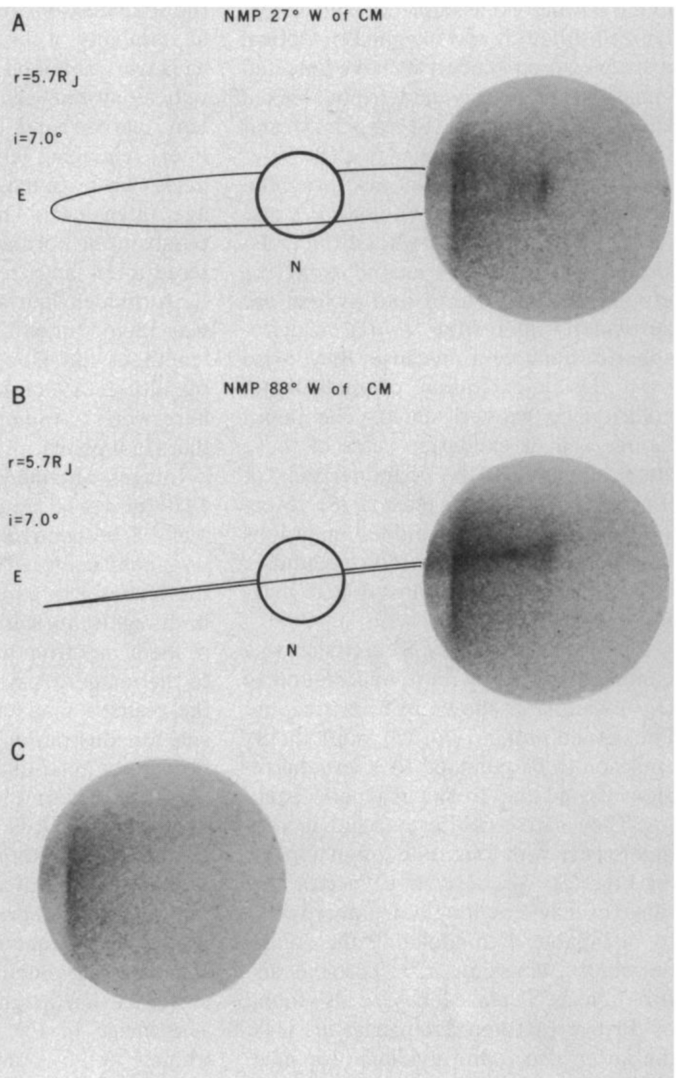

Fig. 1 (left). Images of Jovian sulfur ring obtained in the 6731-Å forbidden line of S^+ on 9 April 1979 (universal time) and a corresponding background image. The schematic associated with each ring image shows Jupiter and a ring of radius $5.3\ R_J$ (*17*) in the Jovian magnetic equator at the mid-time of the 15-minute exposures [*i* is the inclination of the illustrated ring to the rotational equator (*18*)]. The angle in longitude between the north magnetic pole (*NMP*) and the planet's central meridian (*CM*, the great circle passing through the geometric poles and the subearth point) is shown for each ring image. Images A and B were separated by 85 minutes; images B and C, by 29 minutes. Image D shows the same portion of sky as the ring images, but was obtained with the filter detuned so that it passed only the background radiation from Jupiter. Fig. 2 (right). Images obtained as in Fig. 1, but on 10 April 1979 (universal time). A ring of radius $5.7\ R_J$ and inclination 7° to the rotational equator (the inclination of the centrifugal symmetry surface) is shown for comparison with the sulfur ring images. The magnetic longitudes observed in these images are approximately the same as those observed in the images shown in Fig. 1. Image C is a background image obtained with the filter detuned (*25*).

sulfur rings may be stable around Jupiter simultaneously and the emission in each activated by independent, and perhaps nonequilibrium, processes. This possibility is given some credibility by the relative thinness of the ring ($\lesssim 0.3\ R_J$) observed on the first night. If the ring on this night had been composed of hot, newly ionized material, it would have been expected to be substantially thicker (about $2\ R_J$), corresponding to the $\pm\ 10°$ of magnetic latitude traversed by Io in a Jovian rotation (*24*).

CARL B. PILCHER
Institute for Astronomy, University of Hawaii, Honolulu 96822

References and Notes

1. R. A. Brown, *Int. Astron. Union Symp. No. 65* (1974), pp. 527–531; for additional references see C. B. Pilcher and W. V. Schempp, *Icarus* **38**, 1 (1979).
2. L. Trafton, *Nature (London)* **258**, 690 (1975).
3. I. Kupo, Y. Mekler, A. Eviatar, *Astrophys. J.* **205**, L51 (1976).
4. C. B. Pilcher and J. S. Morgan, *Science* **205**, 297 (1979).
5. A. L. Broadfoot *et al.*, *ibid.* **204**, 979 (1979).
6. D. L. Judge, R. W. Carlson, F.-M. Wu, V. G. Hartmann, in *Jupiter*, T. Gehrels, Ed. (Univ. of Arizona Press, Tucson, 1976), pp. 1068–1101.
7. H. S. Bridge, J. W. Belcher, A. J. Lazarus, J. D. Sullivan, R. L. McNutt, F. Bagenal, J. D. Scudder, E. C. Sittler, G. L. Siscoe, V. M. Vasyliunas, C. K. Goertz, C. M. Yeates, *Science* **204**, 987 (1979).
8. R. A. Brown, *Astrophys. J.* **206**, L179 (1976); D. E. Osterbrock, *Astrophysics of Gaseous Nebulae* (Freeman, San Francisco, 1974).
9. Y. Mekler and A. Eviatar, *J. Geophys. Res.* **82**, 2809 (1977).
10. C. B. Pilcher, *Bull. Am. Astron. Soc.* **10**, 579 (1978); J. S. Morgan and C. B. Pilcher, *ibid.*, p. 579.
11. C. B. Pilcher and J. S. Morgan, *Astrophys. J.*, in press.
12. A. J. Dessler and T. W. Hill, *ibid.* **227**, 664 (1979).
13. R. A. Brown, *ibid.* **224**, L97 (1978).
14. J. T. Trauger, G. Münch, F. L. Roesler, *ibid.*, in press.
15. A. Eviatar, G. L. Siscoe, Y. Mekler, *Icarus* **39**, 450 (1979).
16. D. B. Nash, *Eos Trans.* **60**, 307 (1979).
17. The use of R_J here and throughout this report refers to the equatorial radius of the planet.
18. The value $i = 10.6°$ for a ring in the magnetic equator is taken from the Jovian magnetic field model of E. J. Smith, L. Davis, Jr., D. E. Jones, P. J. Coleman, Jr., D. S. Colburn, P. Dyal, and C. P. Sonnett [*J. Geophys. Res* **79**, 3501 (1974)]. The 9° of planetary rotation during an exposure introduced negligible smearing of the images. The nonzero declination of the earth was taken into account in the preparation of the illustrations. At the time of the observations, the rotation axis of the planet was tilted 14° to the celestial north-south direction. This has been ignored for illustrative purposes.
19. *Sci. News* **116**, 155 (1979).
20. G. L. Siscoe, *J. Geophys. Res.* **82**, 1641 (1977).
21. T. W. Hill and F. C. Michel, *ibid.* **81**, 4561 (1976).
22. T. W. Hill, A. J. Dessler, F. C. Michel, *Geophys. Res. Lett.* **1**, 19 (1974).
23. Y. L. Yung, personal communication.
24. G. L. Siscoe and C.-K. Chen, *Icarus* **31**, 1 (1977).
25. The background for observations to the west of the planet is less uniform than for observations to the east because of asymmetric scattering in the telescope.
26. I thank S. Wolff for her lucid thinking at an altitude of 4200 m, and S. Kawamura, E. Enos, and C. Lai for their dedicated work on the design and construction of the instrumentation. A. N. Stockton provided invaluable assistance in mounting the image tube on the new apparatus. A. J. Dessler and G. L. Siscoe helped to guide me through the magnetospheric literature and provided many useful insights. Supported in part by NASA grant NGL 12-001-057.

9 August 1979; revised 12 October 1979

Tectonic Tilt Rates Derived from Lake-Level Measurements, Salton Sea, California

Abstract. *Tectonic tilt at the Salton Sea was calculated by differencing lake-level measurements from two points on the sea. During the past 26 years, tilting was down toward the southeast. By 1970 differential vertical movement amounted to 110 millimeters between two gages situated 38 kilometers apart on the southwest shore. A reversal in tilt direction in late 1972 has diminished the net differential vertical movement to 60 millimeters.*

The discovery by Castle *et al.* (*1*) of significant vertical aseismic tectonic movement over a large region of southern California has led to an examination of records of the vertical geodetic control and a search for other types of geophysical data in order to independently measure and monitor crustal movement in California. Toward this end, we examined records of surface water levels on the Salton Sea taken over the past 26 years.

The Salton Sea occupies the lowest part of the Salton depression, an inland continuation of the Gulf of California (Fig. 1). The altitude of the surface of the Salton Sea is currently about 70 m below sea level. Seasonal lake-level fluctuations are about 0.7 m.

The Salton depression is a large, northwest-trending sedimentary basin that has both downwarped and downfaulted during the late Cenozoic. The greatest thickness of fill in the basin appears to lie about 75 km south of the Salton Sea near the international border, where an estimated thickness of at least 6.4 km of sediments overlies the basement rock. The depth to a Pliocene seismic refractor is estimated to be 4.7 km. The dip of the basement rock under the Salton Sea is down to the southeast (*2*).

The shoreline of a Pleistocene lake that lay along the southwest side of the depression near the international border is reported to have been deformed down to the southeast resulting in a 35-m elevation change over a 24-km littoral distance (1460 μrad of tilt) (*3*). This geophysical and geological evidence suggests that the location of greatest subsidence lay south of the Salton Sea, and that the location of the present lake-filled depression is a result of closure by deltaic sedimentation and not closure by a greater rate of tectonic subsidence.

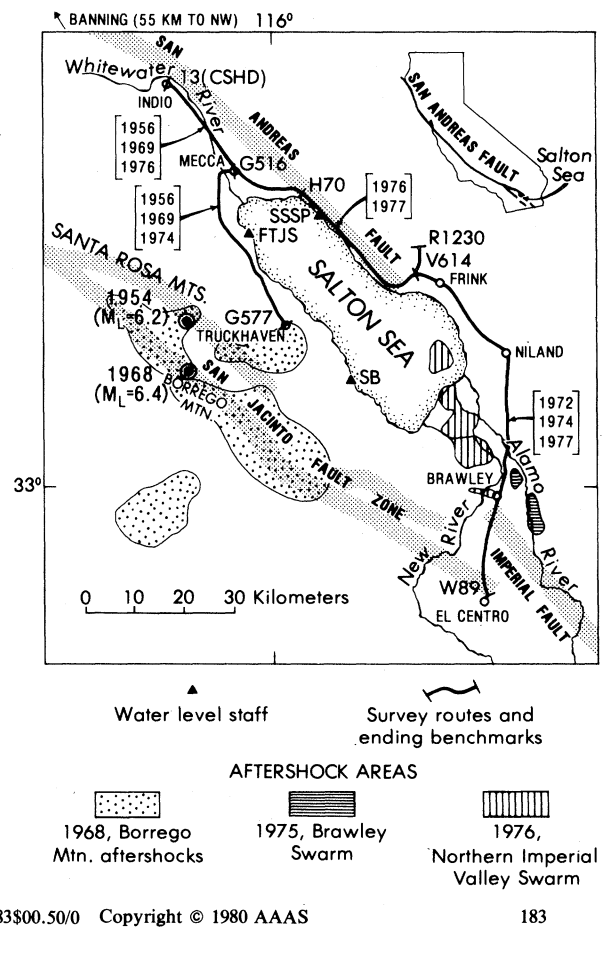

Fig. 1 Map of the Salton Sea area, southern California, showing routes of repeated first-order leveling and locations of terminal benchmarks [13(CSHD), G516, H70, R1230, V614, W89, and G577]. Years in brackets indicate the dates of leveling. The water-level staffs are located at Fig Tree John Springs (*FTJS*), Salton Sea State Park (*SSSP*), and Sandy Beach (*SB*). Locations of the aftershock areas of the 1968 Borrego Mountain earthquake are adapted from Hamilton (*9*). Locations of the 1975 Brawley swarm area are from Johnson and Hadley (*10*), and locations of the 1976 Northern Imperial Valley swarm are from Schnapp and Fuis (*11*); M_L = 6.2 and M_L = 6.4 are Richter magnitudes for moderate-size earthquakes during the years indicated.

0036-8075/80/0111-0183$00.50/0